Neoclassical study of the isotope effect in density pedestals

S. Buller[1], I. Pusztai[1], J.T. Omotani[1], S.L. Newton[2,1]

[1] *Department of Physics, Chalmers University of Technology, SE-41296, Göteborg, Sweden*

[2] *CCFE, Culham Science Centre, Abingdon, Oxon OX14 3DB, UK*

The isotope mass scaling of the energy confinement time in tokamak plasmas typically differs from gyro-Bohm estimates. This phenomenon – known as *the isotope effect* [1] – remains an open issue in plasma physics, with important implications for the extrapolation from present day, mostly deuterium (D), fusion experiments to future deuterium-tritium (D-T) reactors.

Differences in mass scaling in L-mode and various H-mode regimes suggest that the isotope effect may, in large part, originate from the pedestal. In the pedestal, sharp gradients render local diffusive estimates invalid, and global effects due to orbit-width scale profile variations have to be taken into account, potentially leading to mass scalings different from gyro-Bohm.

We calculate cross-field fluxes from a radially-global linearized drift-kinetic equation using the PERFECT code [2], to study isotope composition effects in density pedestals. We define dimensionless parameters from the ratios of density length scale, pedestal width and orbit width, and study global effects in terms of these parameters for different pedestal profiles and bulk species. Quantifying global effects by the relative difference between peak heat-flux values in global and local simulations, we find that this quantity saturates at an isotope-dependent value, but the dimensionless parameters do not capture all the isotope dependencies. We also consider D-T and H-D mixtures, and compare the calculated heat fluxes to fluxes calculated from single-species simulations with artificial "DT" and "HD" species.

Radially global δf drift-kinetics Linearizing the drift-kinetic equation (DKE) of Ref. [3] in $\delta \equiv \rho_p/L$, where $\rho_p = mv/(eB_p)$ is the poloidal gyroradius and L is the equilibrium length-scale, while assuming ρ_p-scale Φ and δf variations, yields the linearized, global DKE [2]

$$(\mathbf{b}v_\parallel + \mathbf{v}_\mathrm{d}) \cdot \nabla g - C_l[g] - S = -\mathbf{v}_m \cdot \nabla f_M, \tag{1}$$

with $g = f - f_M(1 - Ze\tilde{\Phi}/T)$, $\mathbf{v}_\mathrm{d}$ the drift velocity, $\mathbf{v}_m$ the magnetic drift, and $\Phi^t = \Phi + \tilde{\Phi}$ is the total electrostatic potential, with its flux surface average component $\Phi = \langle \Phi^t \rangle$. To account for orbit-width scale potential and g variations, the $\mathbf{v}_\mathrm{d} \cdot \nabla g$ term is retained; it is what differentiates (1) from the conventional local DKE. For the linearization to remain valid, g should be δf_M small. As gradients are taken with $W = mv^2/2 + e\Phi$ and $\mu = mv_\perp^2/(2B)$ fixed, this implies that the temperature T or pseudo-density $\eta = n\mathrm{e}^{e\Phi/T}$ cannot have order unity variations on the

ρ_p-scale. This still allows for strong T_e and η_e variations, due to the small electron orbit-width. The normalization and notation of input and output quantities follow Ref. [4].

Baseline input profiles For the baseline n_e and T_e profiles (shown as functions of the normalized poloidal flux ψ_N in Figure 1), we use mtanh model profiles based on Fig. 1 of Ref. [5]. The T_i and Φ profiles are chosen to yield a weakly varying Maxwellian.

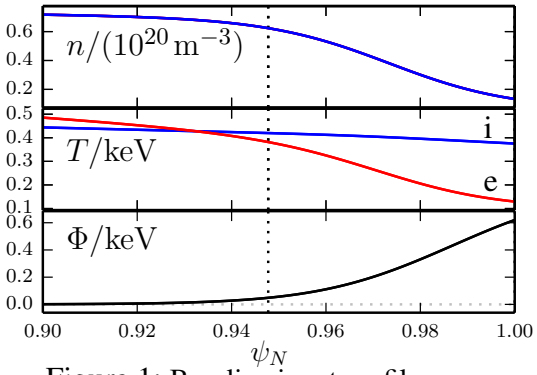

Figure 1: Baseline input profiles.

Heat flux and isotope effect For the baseline input profiles, we calculate the radial fluxes from the global equation (1) and the corresponding local equation – for H, D and T plasma, shown in Figure 2. Global (local) results are indicated by solid (dashed) lines.

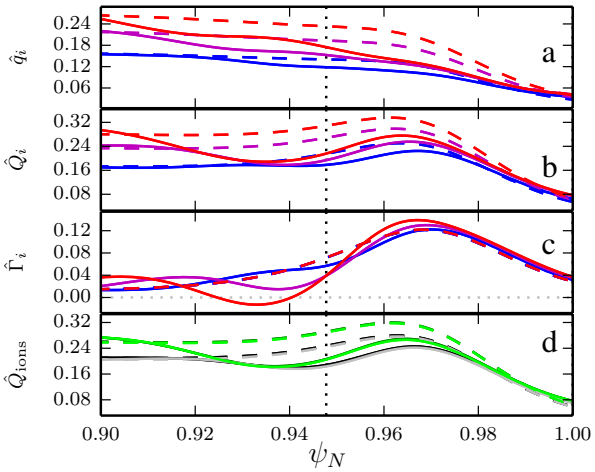

Figure 2: Baseline $\hat{q}_i$ (a), $\hat{Q}_i$ (b), $\hat{\Gamma}_i$ (c), for H [blue], D [purple], T [red] plasma.
d: $\hat{Q}_{\mathrm{ions}}$ for H-D [black] and D-T [green] mixtures and artificial "HD" [gray] and "DT" [lime] species.

For the local results, the conductive heat flux $q = Q - \frac{5}{2}T\Gamma$ is merely rescaled by changing the isotope mass, see Figure 2a. Assuming $q_i = bm_i^{\alpha}$, we obtain $\alpha = 0.42$ (dashed line in Figure 3), roughly consistent with a $\sqrt{m_i}$ mass dependence from analytic banana-plateau results. Note, however, that the convective part of Q is non-negligible in this pedestal, due to the sharp electron profiles. In the local limit, Γ is completely independent of ion mass, leading to a weaker mass scaling of Q_i than that of q_i – see Figure 2b and Figure 2c.

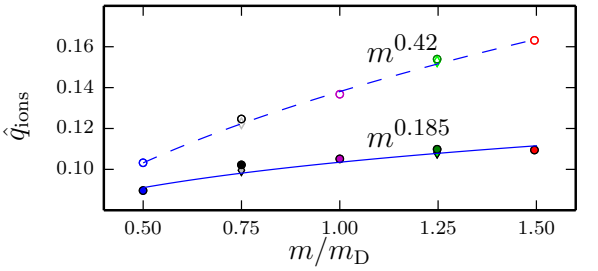

Figure 3: Mid-pedestal $\hat{q}_i$ plotted against the average ion mass and $\hat{q}_i = bm_i^{\alpha}$ fits.

The global particle flux and conductive heat flux in the pedestal are not merely rescaled by changing the isotope mass. For example, the region where global effects modify the fluxes extends into the near-pedestal core over a distance that scales with the orbit width, and indicates the distance over which fluxes in the global simulations are correlated – the *coupling length*. The global Γ_i exhibits a strongly mass-dependent reduction in the near-pedestal core and a weakly mass

dependent increase inside the pedestal. To quantify a mass scaling, we consider the q_i in the middle of the pedestal. Using the same fit for q_i in the middle of the pedestal, we find $q_i \propto m_i^{0.185}$ (solid line in Figure 3).

The non-trivial species effects in global simulations motivate the study of isotope mixtures. Figure 2d shows $\hat{Q}_{\text{ions}} = \sum_i \hat{Q}_i$ in 0.5-0.5 H-D (black) and 0.5-0.5 D-T (green) plasmas, as well as in single species plasmas with artificial "HD" (gray) and "DT" (lime) species with intermediate masses that yield the same mass density as the mixed plasmas. The artificial mass simulations yield good approximations for the heat flux ($\sim 3\%$ rel. error in maxima). This agreement is due to the insensitivity of $\hat{\Gamma}_{\text{ions}}$ to ion mixture and the monotonic behavior of $\hat{q}_i$. The latter property transfers to $\hat{q}_{\text{ions}}$, which thus is qualitatively similar to the single species ion flux. Quantitative differences may be more apparent for higher mass ratios.

Pedestal profile scan As the orbit width sets the scale of the radial coupling, it is interesting to see whether it is possible to predict the extent of global effects, in particular in different isotope plasmas, from dimensionless parameters involving ratios of length scales of the profiles and the orbit width. Let w^{o} be the orbit width in the middle of the pedestal, w the mtanh pedestal width, and L_n^0 the length-scale of the density profile in the middle of the pedestal. Then the dimensionless ratios $\delta_n^* = w^{\text{o}}/L_n^0$ and w^{o}/w may be possible indicators of the size of global effects. These parameters are related by $\delta_n^* = \frac{w^{\text{o}}}{w}\frac{\Delta n}{n_0}$, where $\Delta n/n_0$ is the the relative density drop, $\Delta n/n_0 = (n_{\text{LCFS}} - n_{\text{Ped}})/n_0$. For fixed $\Delta n/n_0$, the above dimensionless ratios are proportional to each other.

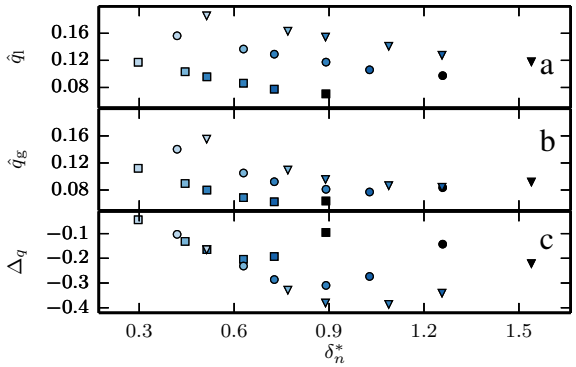

Figure 4: Mid-pedestal $\hat{q}_i$ (a: local, b: global, c: relative difference) for different pedestal widths for different species (square: H, circle: D, triangle: T).

Fixing $\Delta n/n_0$ to the baseline value, we performed simulations with different pedestal widths for our different species. The mid-pedestal $\hat{q}_i$ for local ($\hat{q}_{\text{l}}$) and global ($\hat{q}_{\text{g}}$) simulations are shown in Figure 4; the different species are indicated by different symbols. For each isotope, sharper density pedestals yield lower local values, while the global values saturate and slightly increase beyond species dependent thresholds in δ_n^*. This is most easily seen in Figure 4c, which depicts the relative difference $\Delta q = \hat{q}_{\text{g}}/\hat{q}_{\text{l}} - 1$, which initially decreases with δ_n^*, but then starts to go up to zero as the global fluxes are saturated. If the relative difference is taken as a measure of global effects, the different species not lining up in Figure 4c implies that global isotope effects cannot be accounted for by rescaling the profiles to compensate for different orbit widths.

Similarly, the global particle flux (Figure 5) first increases with δ_n^* faster than the local fluxes, but then become less sensitive to δ_n^* (they do not saturate though) while the local fluxes are essentially linear and eventually overtake the global fluxes for larger δ_n^*. Particle fluxes show only a weak isotope dependence: the different slopes for each isotope are due to the mass dependence in δ_n^* and thus artificial. In conclusion, δ_n^* is not predictive of global effects, although they are correlated.

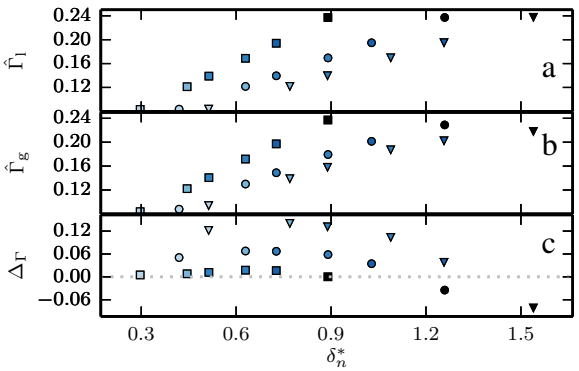

Figure 5: Plots corresponding to Figure 4, but for the peak value of particle fluxes in the pedestal.

Thus, δ_n^* does not capture the full isotope dependence of global effects on the conductive or convective parts of the heat flux, even when $\Delta n/n_0$ is kept fixed. For low values of δ_n^*, the relative difference between global and local fluxes may scale linearly with δ_n^*, but the region of validity for this scaling depends on the isotope. These results are backed up by more numerous simulations in Ref. [6], where the dependence of $\hat{Q}_i$ on $\Delta n/n_0$ is also considered.

Conclusions We have shown that isotope mixtures to some extent can be mocked up by a single species with an intermediate, effective mass, for the purpose of calculating global neoclassical heat-fluxes. Furthermore, we have shown that the global effects due to changing isotope in our simulations cannot be accounted for by simply rescaling pedestal width or density length scale to compensate for the different orbit widths, but that Γ_i is mostly independent of mass and that the global q_i fluxes saturate at a species dependent δ_n^*. When the convective heat flux is large enough to be comparable to the conductive heat flux, which may occur when T_e but not T_i has a pedestal, even local heat fluxes show a non-trivial mass dependence. Thus main ion temperature pedestal measurements may be important for isotope effect studies in the pedestal.

Acknowledgments SB and IP were supported by the INCA grant of Vetenskapsrådet (Dnr. 330-2014-6313). JO and SN by the Framework grant for Strategic Energy Research (Dnr. 2014-5392). Simulations used resources of Hebbe at C3SE (SNIC2016-1-161 & SNIC2017-1-95) and Kebnekaise at HPC2N (SNIC2017-3-29).

References

[1] I. Pusztai, J. Candy, P. Gohil, Physics of Plasmas **18**, 122501 (2011).
[2] M. Landreman, et al., Plasma Phys. Control. Fusion **56**, 045005 (2014).
[3] R.D. Hazeltine, Plasma Physics **15**, 77 (1973).
[4] S. Buller, I. Pusztai, S.L. Newton, J.T. Omotani, Plasma Phys. Control. Fusion **59**, 055019 (2017).
[5] E. Wolfrum, et al., Nuclear Fusion **55**, 053017 (2015).
[6] S. Buller, I. Pusztai, "Isotope and density profile effects on pedestal neoclassical transport" https://arxiv.org/abs/1705.06762